Electronic Supporting Information for

High-yield and in-situ fabrication of high-content nitrogen-doped graphene nanoribbons@Co/CoOOH as an integrated sulfur host towards Li-S batteries

*Ke Tan†, Yang Liu†, Zhaolin Tan, Jinyang Zhang, Linrui Hou and Changzhou Yuan**

School of Materials Science & Engineering, University of Jinan, Jinan, 250022, P. R. China

E-mail: ayuancz@163.com; mse_yuancz@ujn.edu.cn

† Theses authors contributed equally to this work.

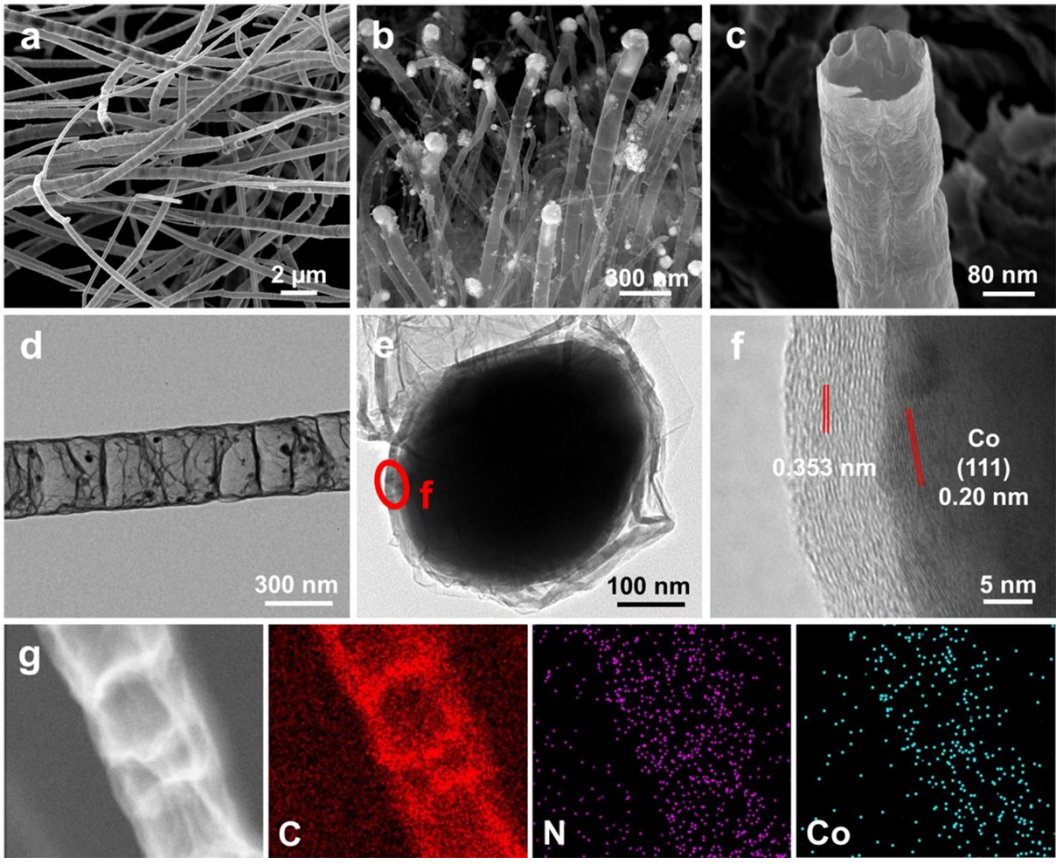

Fig. S1 (a-c) FESEM, (d, e) TEM, (f) TEM images of the N-CNTs@Co and (g) EDX elemental mapping images of the N-CNTs@Co. It is clear that the N-CNTs@Co have bamboo-like structure, the cobalt nanoparticles at the top of N-CNTs and smaller cobalt nanoparticles distributed inside the N-CNTs@Co

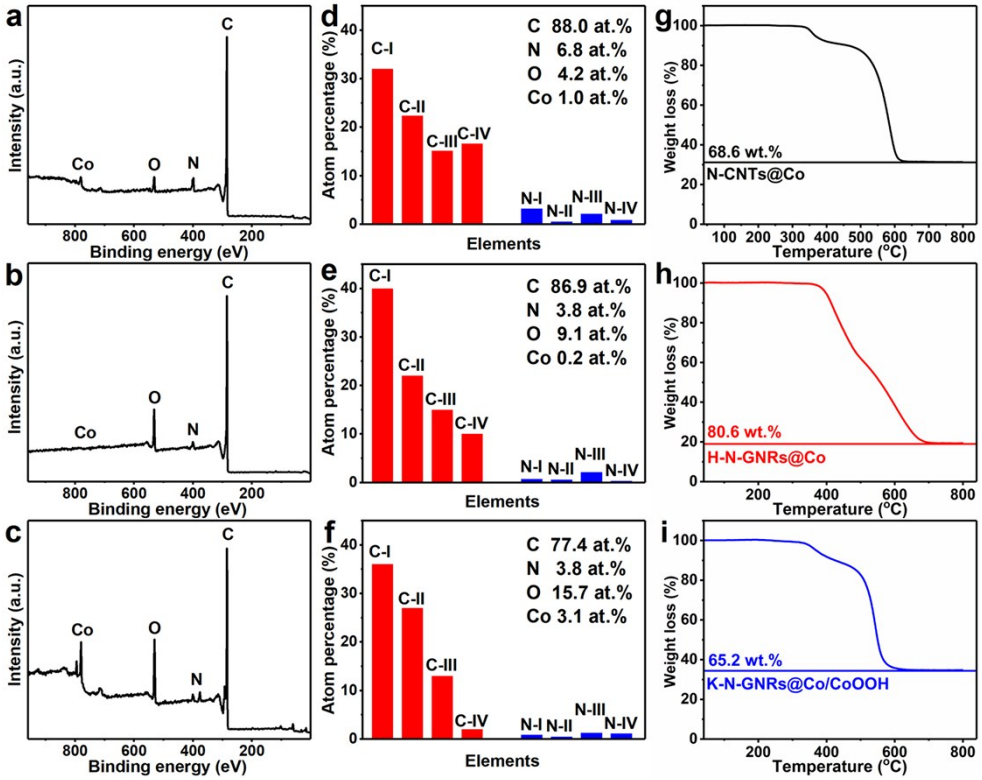

Fig. S2 Typical XPS survey spectrum of the (a) N-CNTs@Co (above), (b) H-N-GNRs@Co (middle) and (c) K-N-GNRs@Co/CoOOH (bottom); Relative content profiles of di□erent types of carbon and nitrogen atoms in the (d) N-CNTs@Co (above), (e) H-N-GNRs@Co (middle) and (f) K-N-GNRs@Co/CoOOH (bottom) and TGA curves of (g) N-CNTs@Co (above), (h) H-N-GNRs@Co (middle) and (i) K-N-GNRs@Co/CoOOH (bottom)

After conversion calculation from Co_3O_4 and Co, the carbon content in the K-N-GNRs@Co/CoOOH and contrastive samples (N-CNTs@Co, H-N-GNRs@Co) have been calculated to be 77.0 wt.% (N-CNTs@Co), 85.8 wt.% (H-N-GNRs@Co) and 74.5 wt.% (K-N-GNRs@Co/CoOOH) *via* TG analysis (Fig. S2g-i).

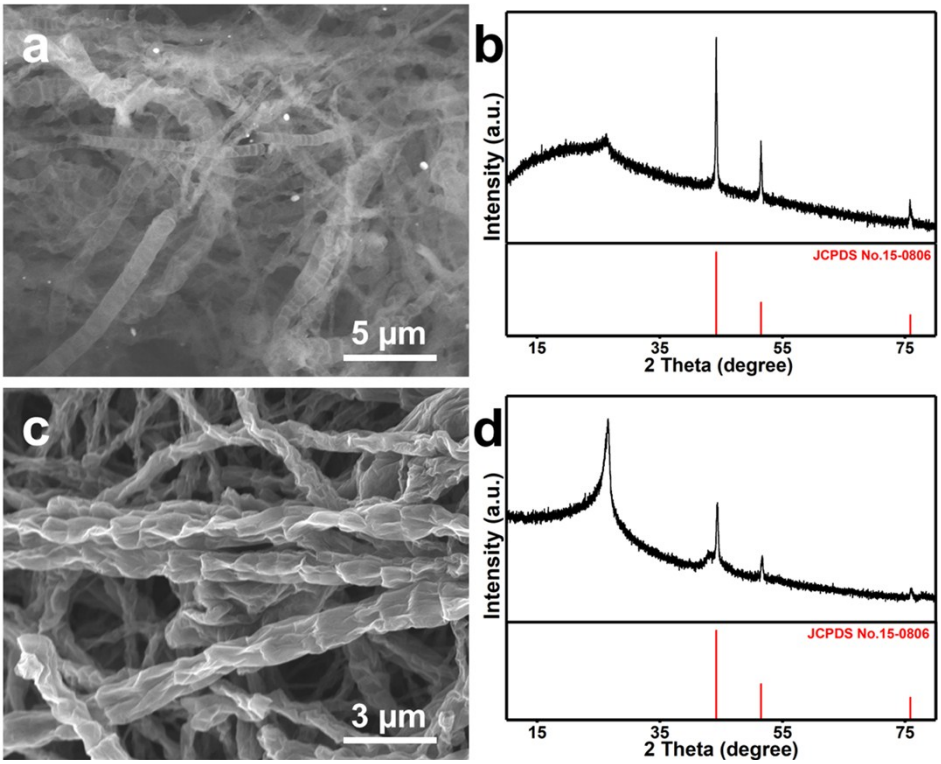

Fig. S3 (a) SEM images and (b) XRD patterns of the N-CNTs@Co immersed in 6 M HNO_3 for 6 h at 50 °C; (c) SEM images and (d) XRD patterns of the N-CNTs@Co immersed in 6 M HNO_3 for 6 h at 70 °C

Obviously, the N-CNTs@Co cannot be unzipped effectively at a lower temperature of 50 °C (**Fig. S3**a). Besides, the typical diffraction peaks for metal Co (JCPDS No. 15-08-06), the weak signal at 26.5 ° for the (002) plane of the graphitic carbon can be observed in **Fig. S3**b, which indicating the amorphous carbon cannot be etched from the N-CNTs@Co at such condition. While with the temperature increasing to 70 °C, the N-CNTs@Co is unzipped thoroughly (**Fig. S3**c), and graphitization degree is improved significantly as the (002) peak turns out to be even strong (**Fig. S3**d), suggesting the high-content amorphous carbon have been etched well by 6 M HNO_3 at 70 °C for 6 h. Moreover, the intensity of the Co signal becomes weaker, revealing more metallic Co has been removed from the N-CNTs@Co with the unzipping temperature increasing.

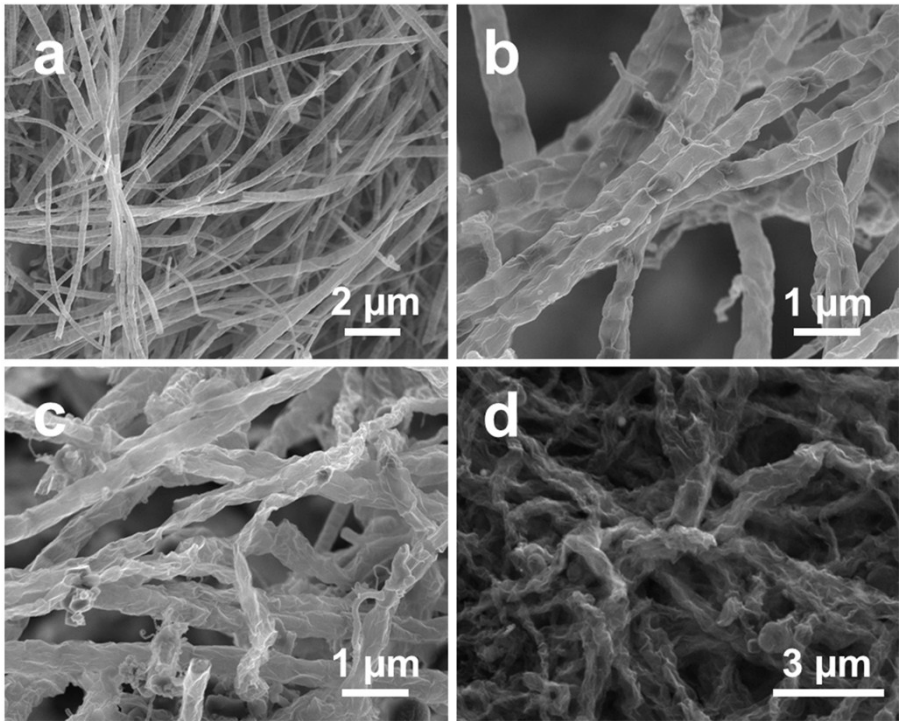

Fig. S4 SEM images of the N-CNTs@Co immersed in HNO_3 solutions with different concentrations: (a) 2 M, (b) 4 M, (c) 8 M and (d) 16 M

Interestingly, the concentration of the aqueous HNO_3 hugely influences the final structure of the products, and the soaking temperatures are all kept at 60 °C for 6h. As for the case of the HNO_3 unzipping process, the N-CNTs@Co cannot be well unzipped with the 2 M (**Fig. S4**a) and 4 M (**Fig. S4**b) HNO_3, while the high-concentration 8 M (**Fig. S4**c) and 16 M (**Fig. S4**d) HNO_3 obviously destroy its unique 1D morphology. Thus, the approximate soaking concentration is chosen as 6 M.

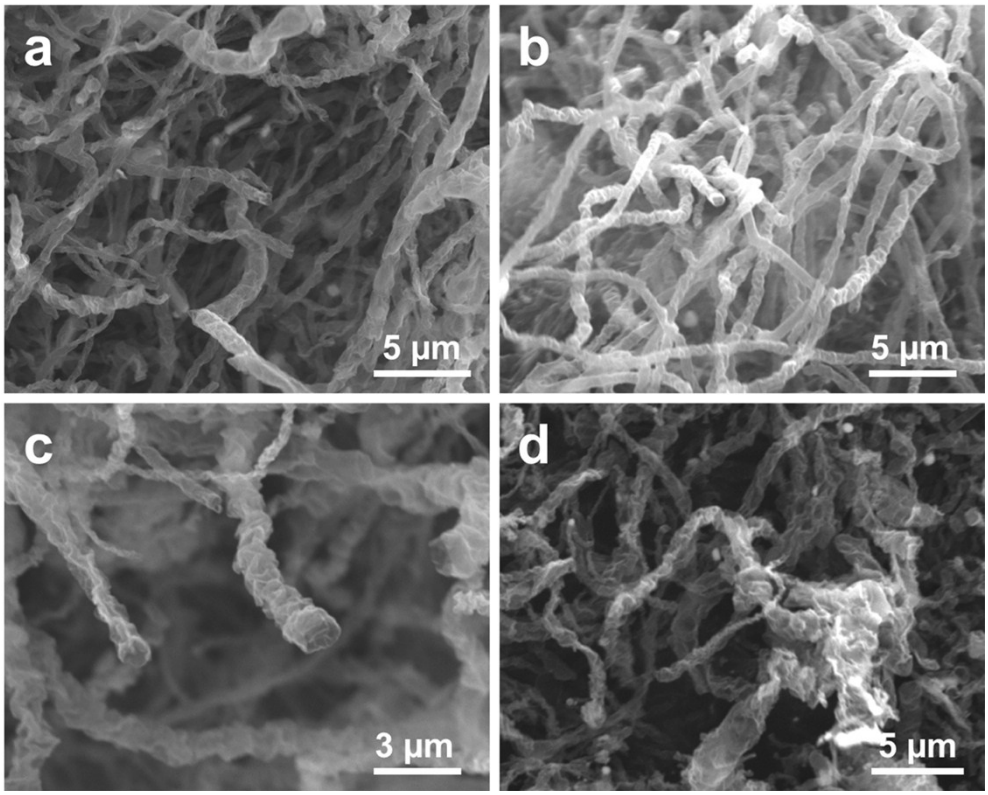

Fig. S5 SEM images of the N-CNTs@Co immersed in 6 M HNO_3 solution at 60 °C for (a) 2 h and (b) 4 h

When the soaking time is lower than 6h, it is obviously that N-CNTs@Co could not be well unzipped (2 h, **Fig. S5**a; 4 h, **Fig. S5**b). And if the soaking time was prolonged to 8 h (**Fig. S5**c), some GNRs can be observed. But the nanoribbons structure would be seriously destroyed as the soaking time was further extended to 12 h (**Fig. S5**d).

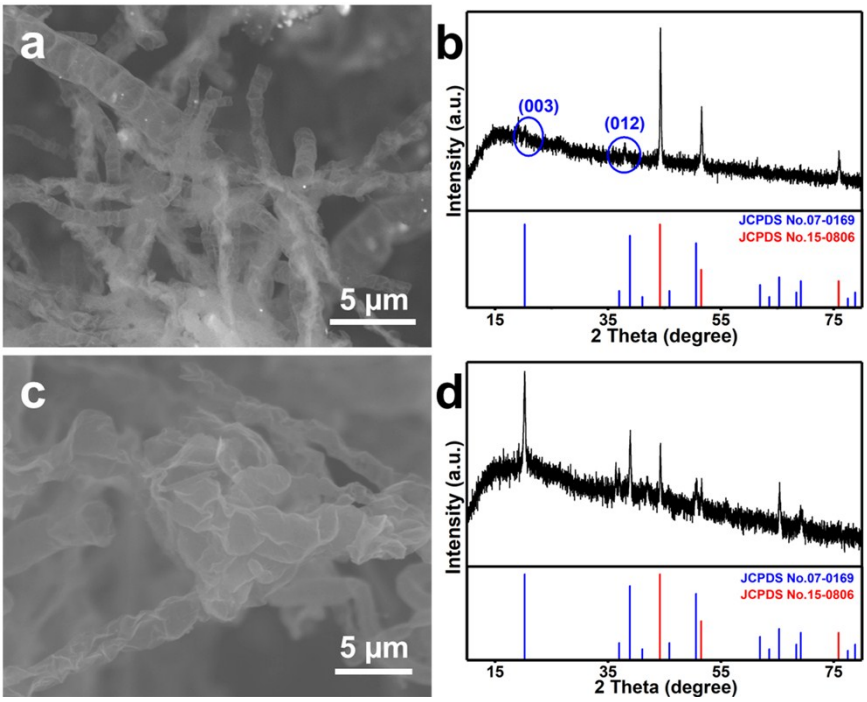

Fig. S6 (a) SEM images and (b) XRD pattern of the N-CNTs@Co immersed in 10 M KOH solutions for 6 h at 80 °C; (c) SEM images and (d) XRD pattern of the N-CNTs@Co immersed in 10 M KOH solution for 6 h at 100 °C

Similarly, the N-CNTs@Co could not be well unzipped at a lower temperature of 80 °C (**Fig. S6a**), and just a little CoOOH (JCPDS No. 07-0169) appears (**Fig. S6b**), except the metal Co. In contrast, some large CoOOH nanosheets emerge after being unzipped at 100 °C for 6 h besides the 1D N-GNRs (**Fig. S6c**, **S6d**).

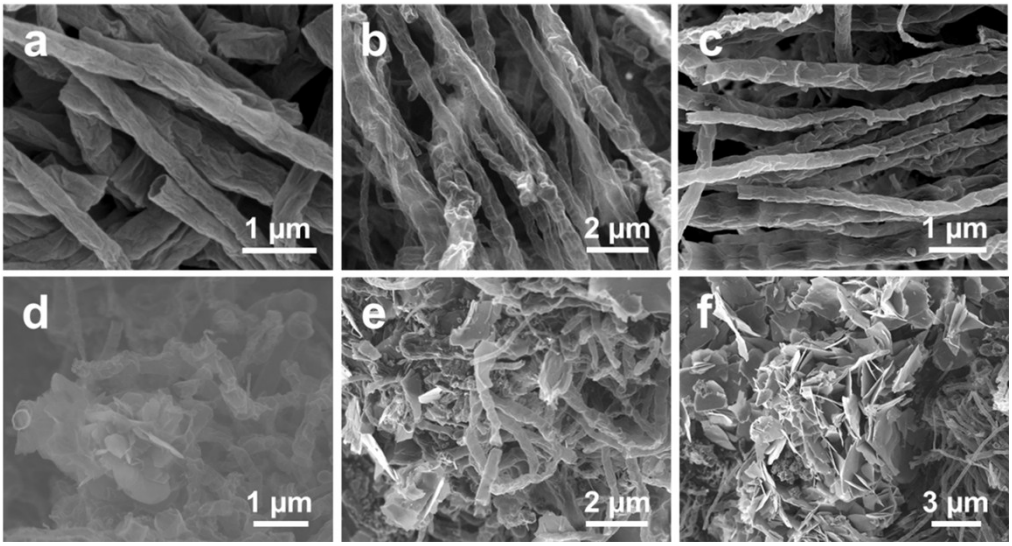

Fig. S7 SEM images of the N-CNTs@Co immersed in (a) 5 M, (b) 8 M, (c) 9 M, (d) 11 M, (e) 12 M and (f) 15 M KOH solutions at 90 °C for 6 h

As regards the KOH unzipping cases, we explored the influence of KOH solution concentrations (**Fig. S7**). Evidently, the low-concentration KOH solution (5 M) cannot result in the successful formation of the nanoribbon structure, and most of them are still NTs (**Fig. S7**a). As the concentration is increased to 8 M (**Fig. S7**b) and 9 M (**Fig. S7**c), more and more nanoribbon-like structure could be found. But with the concentration of KOH solution is higher than 10 M, partial CoOOH nanosheets appear in the sample after treated by 11 M KOH solution (**Fig. S7**d), and more nanosheets of even larger size are observed when the concentration increased to 12 M (**Fig. S7**e). More interestingly, when the KOH concentration is up to 15 M, almost whole nanosheets can be observed (**Fig. S7**f).

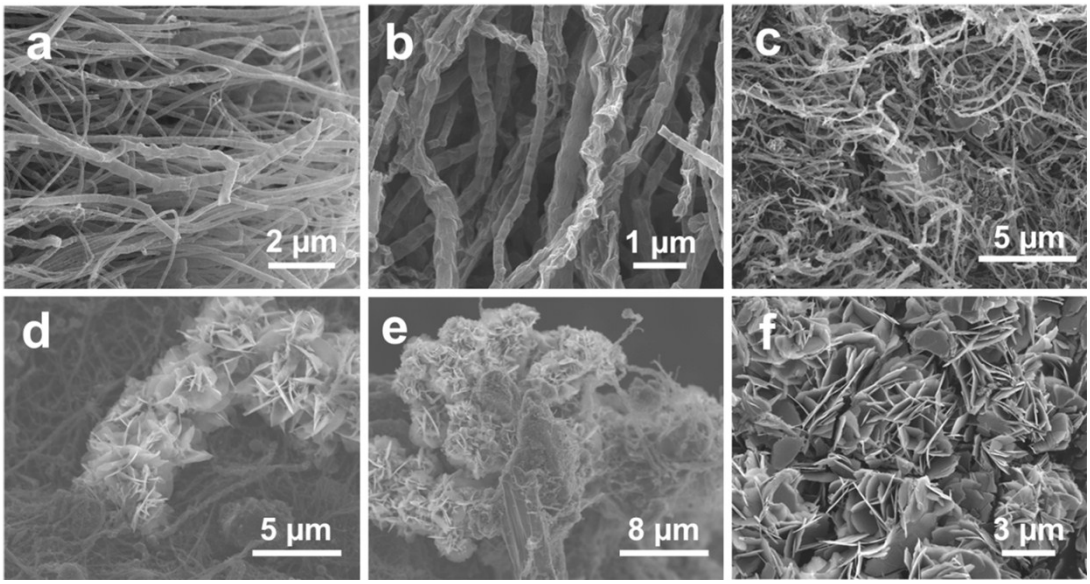

Fig. S8 SEM images of the N-CNTs@Co immersed in 10 M KOH solutions at 90 °C for different times: (a) 2 h, (b) 4 h, (c) 8 h, (d) 12 h, (e) 16 h and (f) 24 h

For the influence of the unzipping time, the N-CNTs@Co is soaked in 10 M KOH solutions for 2 h, 4 h, 8 h, 12 h, 16 h and 24 h, respectively, at 90 °C. As for the case of 2 h (**Fig. S8**a), a little N-CNTs@Co can be unzipped. And more GNRs are observed as the time prolongs to 4 h (**Fig. S8**b). But when soaked for 8 h, extra CoOOH nanosheets are obvious (**Fig. S8**c), and these nanosheets grow even bigger as the time increases to 12 h (**Fig. S8**d). For a longer soaked time, just a little GNRs are visualize after 16 h (**Fig. S8**e) and with further unzipping for 24 h (**Fig. S8**f), nearly all the CoOOH nanosheets emerge, and no any 1D structures can be observed.

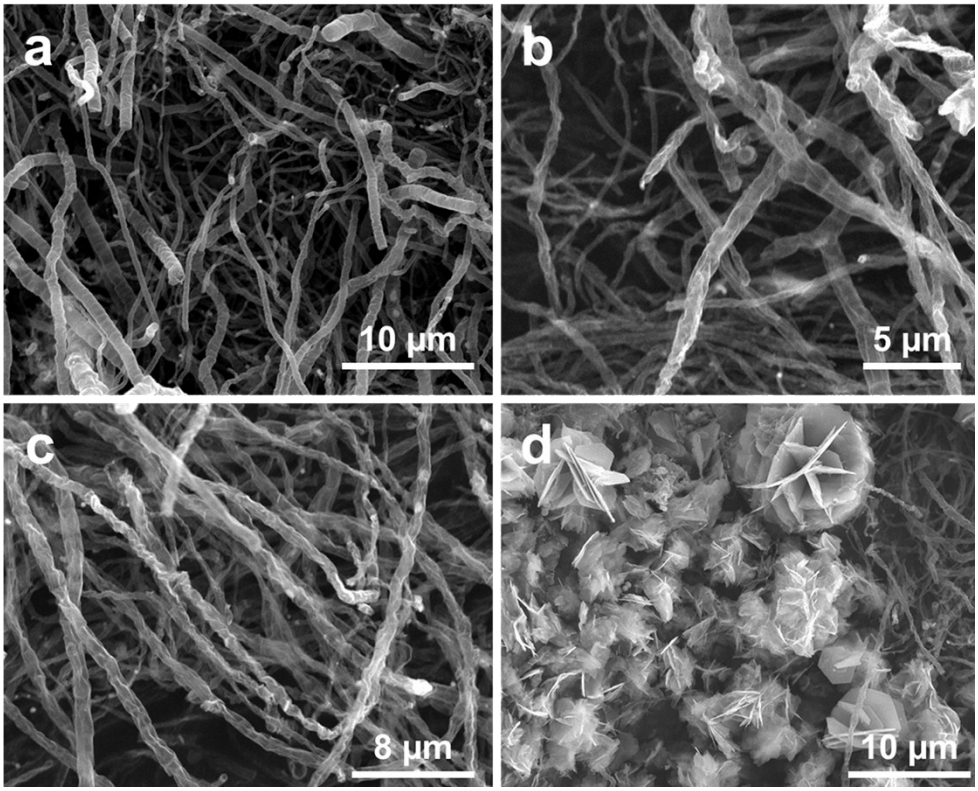

Fig. S9 SEM images of N-CNTs@Co immersed in 10 M KOH solutions at room temperature for (a) 6 h, (b) 12 h, (c) 18 h and (d) 24 h

For the unzipping of N-CNTs@Co by KOH solutions, we found that N-CNTs@Co also could be partially unzipped at room temperature (**Fig. S**9). When being soaked for 6 h, the N-CNTs@Co is not obviously been unzipped (**Fig. S**9a), and be partly unzipped as the time was prolonged to 12 h (**Fig. S**9b) and 18h (**Fig. S**9c). But if further extended the unzipping time, distinct huge CoOOH nanosheets would appear (**Fig. S**9d).

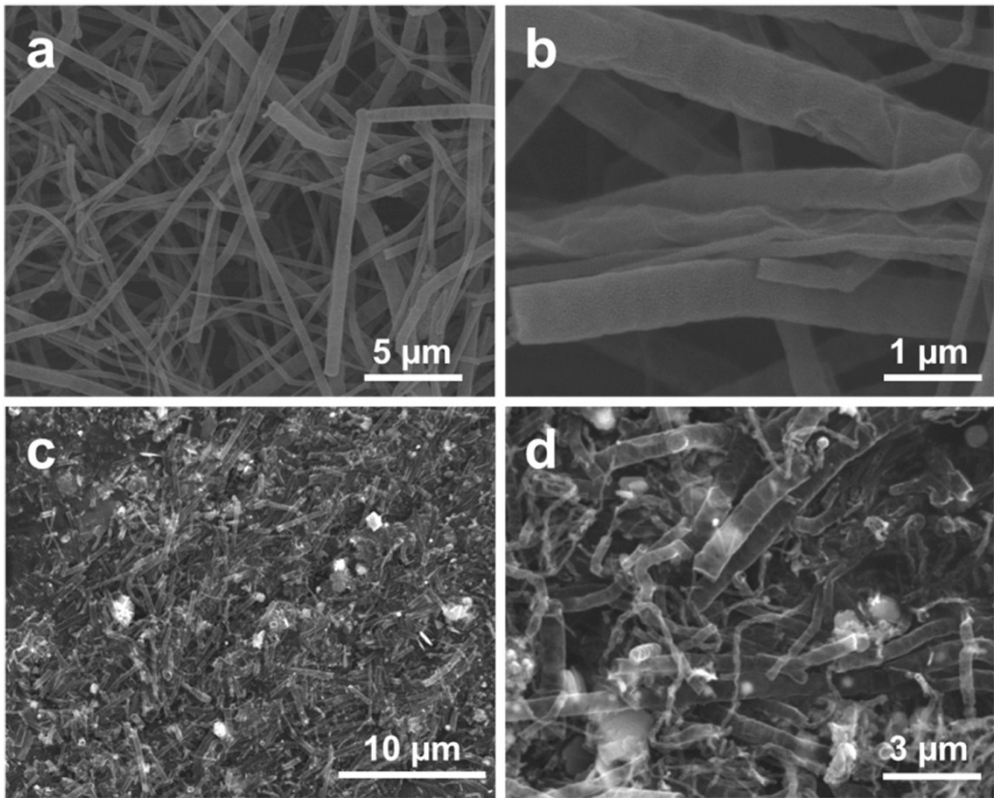

Fig. S10 SEM images of (a, b) the fresh N-CNTs@Co-1000 and (c, d) after immersed in 10 M KOH solution at 90 °C for 6 h

In addition, when the degree of graphitization of such carbon nanotubes is higher, the KOH solution cannot be unzipped. **Fig. S**10 shows SEM images of the N-CNTs@Co-1000 (**Fig. S10**a, b) and those after etched by KOH solutions (**Fig. S10**c, d). It can be seen that when the degree of graphitization is higher, the KOH solution just can cut the N-CNTs into small segments without unzipping.

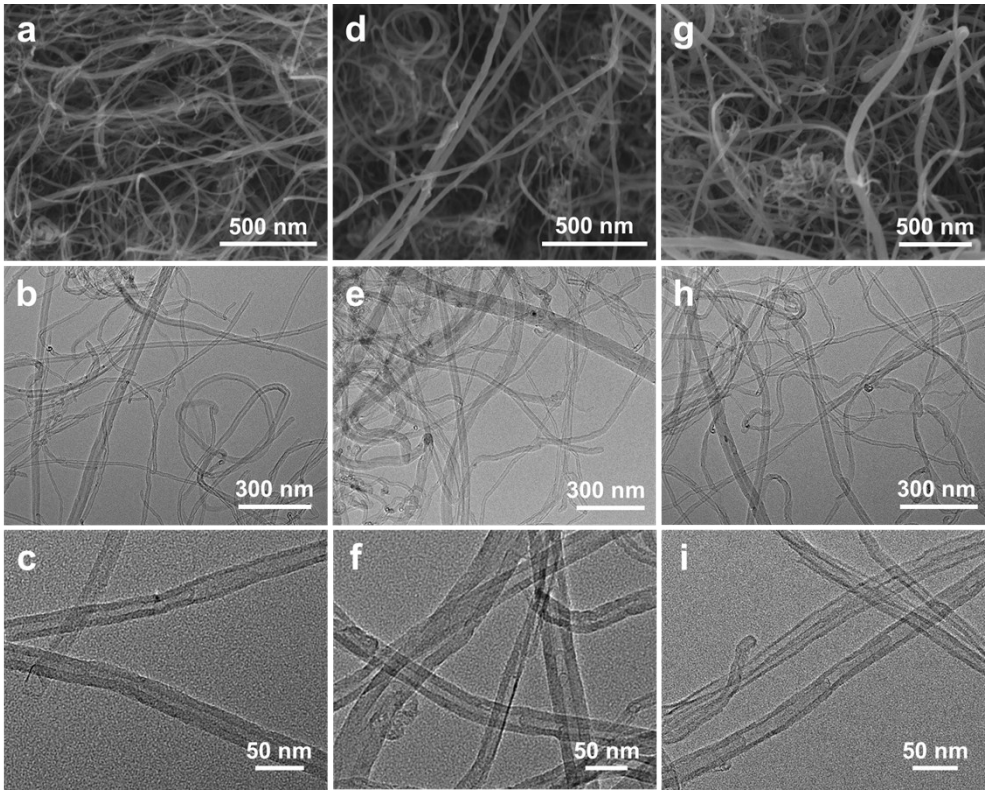

Fig. S11 (a) FESEM image and (b, c) TEM images of commercial CNTs, (d) FESEM image and (e, f) TEM images of commercial CNTs immersed in 6M HNO_3 solutions for 6h at 60 ºC, (g) FESEM image and (h, i) TEM images of commercial CNTs immersed in 10 M KOH solutions for 6 h at 90 ºC

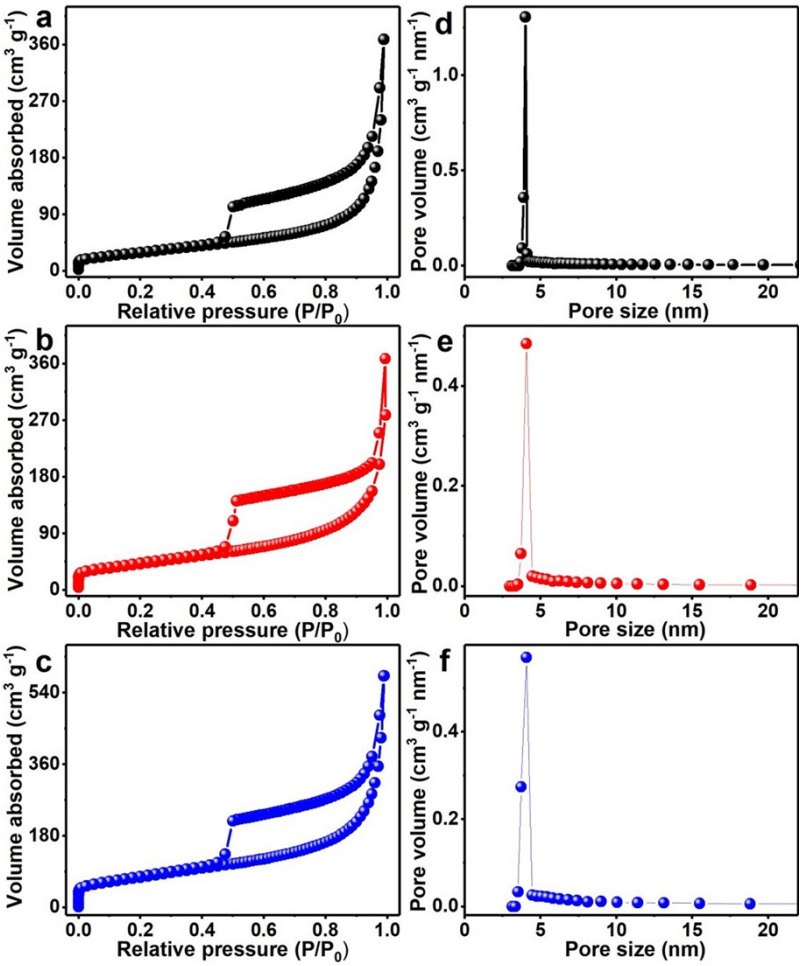

Fig. S12 (a – c) N_2 adsorption-desorption isotherms and (d – f) pore size distribution plots of (a, d) N-CNTs@Co (the upper), (b, e) H-N-GNRs@Co (the middle) and (c, f) K-N-GNRs@Co/CoOOH (the lower)

Table S1 Total pore volume, average pore size and BET SSA of the N-CNTs@Co, H-N-GNRs@Co and K-N-GNRs@Co/CoOOH

Materials	Pore volume ($cm^3\ g^{-1}$)	Average pore size (nm)	BET SSA ($m^2\ g^{-1}$)
N-CNTs@Co	0.37	2.02	112.6
H-N-GNRs@Co	0.57	9.71	150.6
K-N-GNRs@Co/CoOOH	0.90	13.19	273.3

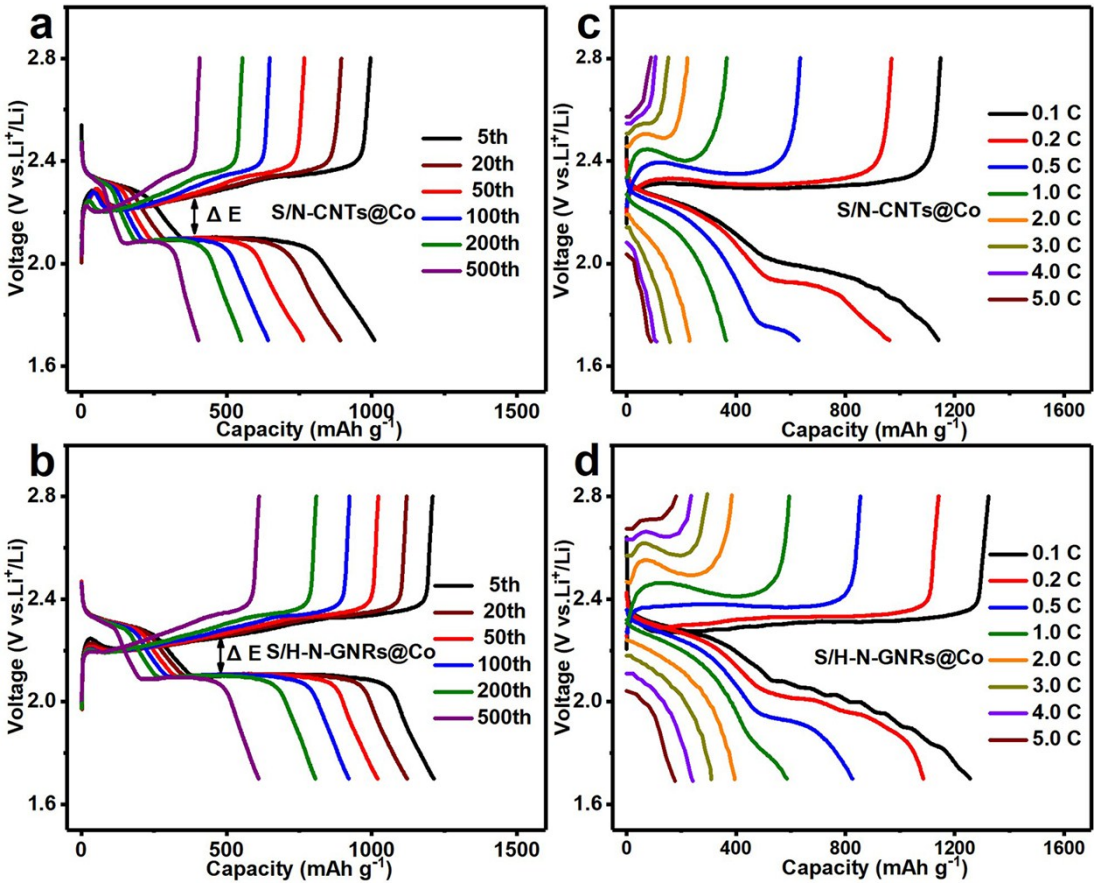

Fig. S13 The galvanostatic charge and discharge voltage profiles of (a) S/H-N-GNRs@Co, (b) S/N-CNTs@Co electrodes for selected cycles; The galvanostatic charge and discharge voltage profiles at different current densities from 0.1 C to 5 C of (c) S/H-N-GNRs@Co and (d) S/N-CNTs@Co

Table S2 Electrochemical collection of the S/N-CNTs@Co, S/H-N-GNRs@Co and S/K-N-GNRs@Co/CoOOH electrodes

Cathodes	S content (wt.%)	Initial capacity (mAh g^{-1})	Capacity after 500 cycles (mAh g^{-1})	Decay per cycle	Rate capability (mAh g^{-1} at 5 C)
S/N-CNTs @Co	63.5	1009.3	400.7	0.12%	86
S/H-N-GNRs@Co	68.2	1257.7	608.0	0.10%	182
S/K-N-GNRs@Co/CoOOH	73.7	1195.6	804.9	0.06%	533

Table S3 Electrochemical performance of the S/K-N-GNRs@Co/CoOOH with different areal S loadings at 0.5 C

Areal S loading	Initial capacity	After 1000 cycles	Decay per cycle
1.1 mg cm^{-2}	1328.7 mAh g^{-1}	558.9 mAh g^{-1}	0.06%
3.9 mg cm^{-2}	1139.3 mAh g^{-1}	516.7 mAh g^{-1}	0.05%

Table S4 Comparison of battery properties of S/K-N-GNRs@Co/CoOOH and other S-based cathodes (1C = 1650 mA g^{-1})

Electrodes	Sulfur content (wt.%)	Cycling stability	Rate capability	Reference
S/K-N-GNRs@Co/CoOOH	73.7	804.9 mAh g^{-1} after 500 cycles at 0.2 C	533 mAh g^{-1} at 5.0 C	This work
S/CoOOH	68.2	788.4 mAh g^{-1} after 100 cycles at 0.2 C	535 mAh g^{-1} at 2.0 C	[1]
S/GN–CNT	76.4	639.1mAh g^{-1} after 200 cycles at 0.1 C	408 mAh g^{-1} at 2.0 C	[2]
S/UZ.CNTs	51.0	707.2 mAh g^{-1} after 60 cycles at 0.2 C	530 mAh g^{-1} at 2.0 C	[3]
S/NBCGN	65.0	740.0 mAh g^{-1} after 300 cycles at 0.2 C	400 mAh g^{-1} at 4.0 C	[4]
S/MWNT-OH25	66.0	720.0 mAh g^{-1} after 100 cycles at 0.1 C	400 mAh g^{-1} at 2.0 C	[5]
S/ACT@Fe/Fe3C	50.0	466.0 mAh g^{-1} after 600 cycles at 0.4 C	440 mAh g^{-1} at 0.4 C	[6]
C–Co-S	66.6	643.0 mAh g^{-1} after 300 cycles at 0.18 C	479 mAh g^{-1} at 5.0 C	[7]
S/NP-TiO@C	73.0	680.0 mAh g^{-1} after 400 cycles at 0.2 C	620 mAh g^{-1} at 2.0 C	[8]

Note: S/CoOOH: nano-sulfur/CoOOH nanosheets; S/GN-CNT: nano-sulfur/CNTs in-situ formed on graphene nanosheets; S/UZ.CNTs: sulfur/unzipped CNTs; S/NBCGN: sulfur/N, B co-doped curved graphene nanosheets; S/MWNT-OH25: sulfur/hydroxylated MWCNTs; S/ACT@Fe/Fe_3C: sulfur/activated cotton textile@ Fe/Fe_3C nanoparticles; C-Co-S: sulfur/Co-doped porous carbon; S/NP-TiO@C: sulfur/titanium monoxide@carbon.

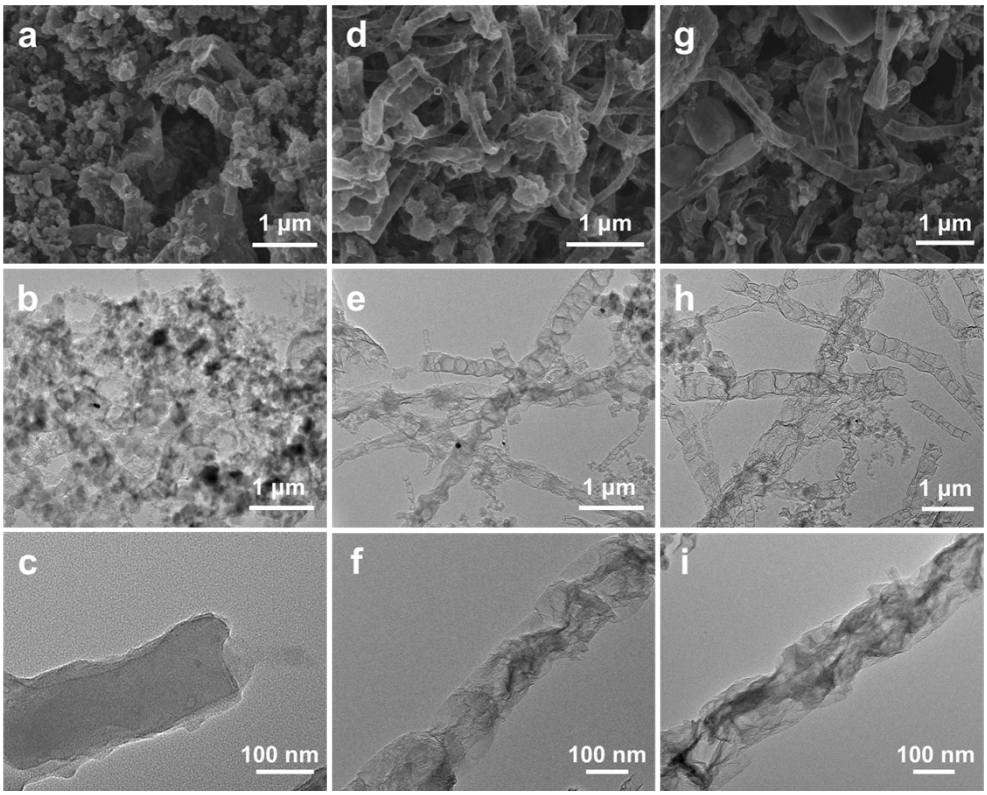

Fig. S14 (a) FESEM image and (b, c) TEM images of N-CNTs, (d) FESEM image and (e, f) TEM images of H-N-GNRs@Co, (g) FESEM image and (h, i) TEM images of K-N-GNRs@Co/CoOOH after cycling

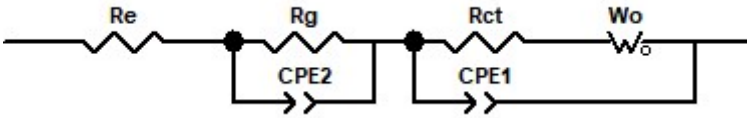

Fig. S15 The equivalent circuit mode used to fit the EIS spectra of the S/N-CNTs@Co, S/H-N-GNRs@Co and S/K-N-GNRs@Co/CoOOH

Table S5 Fitted data of EIS spectra of the fresh S/N-CNTs@Co, S/H-N-GNRs@Co and S/K-N-GNRs@Co/CoOOH cathodes

Cathodes	R_e/ohm	R_{ct}/ohm	R_g/ohm	W_o/ohm
S/N-CNTs@Co	5.9	158.6	116.2	533.8
S/H-N-GNRs@Co	5.5	26.6	32.1	170.2
S/K-N-GNRs@Co/CoOOH	3.3	22.5	10.7	110.1

References

[1] Z. Wang, L. Wang, S. Liu, G. Li and X. Gao, *Adv. Funct. Mater.,* **2019**, 29, 1901051.

[2] Z. Zhang, L. Kong, S. Liu, G. Li and X. Gao, *Adv. Energy Mater.,* **2017**, 7, 1602543.

[3] Y. Jeong, K. Lee, T. Kim, J. Kim, J. Park, Y. Cho, S. Yang and C. Park, *J. Mater. Chem. A,* **2016**, 4, 819.

[4] L. Chen, J. Feng, H. Zhou, C. Fu, G. Wang, L. Yang, C. Xu, Z. Chen, W. Yang and Y. Kuang, *J. Mater. Chem. A,* **2017**, 5, 7403.

[5] J. Kim, K. Fu, J. Choi, S. Sun, J. Kim, L. Hu and U. Paik, *Chem. Commun.,* **2015**, 51, 13682.

[6] Z. Gao, Y. Schwab, Y. Zhang, N. Song and X. Li, *Adv. Funct. Mater.,* **2018**, 28, 1800563.

[7] Z. Li, C. Li, X. Ge, J. Ma, Z. Zhang, Q. Li, C. Wang and L. Yin, *Nano Energy,* **2016**, 23, 15.

[8] Z. Li, B. Guan, J. Zhang and X. Lou, *Joule,* **2017**, 1, 576.